Automatic Lesion Tracking in Echo-Planar Diffusion-Weighted Liver MRI: An Active Contour Based Approach

C. Krishnamurthy[1], J. Rodriguez[1], N. Raghunand[1], R. Theilmann[2], N. Rajguru[1], R. Gillies[1]

[1]University of Arizona, Tucson, AZ, United States, [2]University of California, San Deigo, CA, United States

Abstract. We present an algorithm for automated tracking of liver metastatic lesions across different b-values (from 150-300 s/mm^2) in echo-planar diffusion-weighted magnetic resonance images (EP-DWI). The proposed algorithm for lesion tracking is based on active contours (snakes). The initialization for the active contour model used for tracking was determined using the contour describing the lesion on the b-450 s/mm^2 data set as the reference. Using this initialization, the contour outlining the corresponding lesion on the b-300 s/mm^2 data set was obtained using first moments, block matching and active contour deformation. The same procedure was applied to track the corresponding lesion in the b-150 s/mm^2 data set using the contour from the b-300 s/mm^2 data set as the reference. Segmented lesions were compared to radiologist defined ROIs and were shown to provide an accurate representation of the lesion boundary at different b-values.

Introduction. Diffusion-weighted MRI has gained importance as a non-invasive and early biomarker for anti-cancer chemotherapies [1]. However, motion between scans at different b-values, especially in liver lesions hinders the direct application of pixel-by-pixel image analysis schemes. Many methods have been proposed and implemented to correct image misalignments caused by breathing and other physiological effects. Methods based on the first principle have used correlation as a measure to match two regions [2]. This approach did not work well with the images in our study, since the substantial amount of noise could make the process of correlation peak selection unreliable. Modeling the motion in terms of a fixed parametric equation [3] was also not effective due the varying rigid and non-rigid motions in our samples. Moreover, the feedback mechanism to update the governing equation was computationally expensive. We found that the use of first moments for motion estimation was not sufficient. Similarly, Fourier methods [4] did not perform well with these images, possibly due to the influence of sharp edges. Optical flow based algorithms [5] and Kalman filter based schemes [6] were computationally expensive. The algorithm proposed here combined the rigid motion tracking capabilities of first moments and deformation-tracking capabilities of block matching, based on maximum absolute differences. The resulting tracking algorithm did not require manual ROI selection or seed points.

Methods. The study consisted of diffusion-weighted echo-planar images liver (figure 1, 128x128 matrix, 6mm slice thickness) acquired on a 1.5T GE Signa scanner from patients undergoing treatment for metastatic breast cancer [7]. The block diagram for the proposed segmentation approach is shown in fig. 2. The contour on the b-450 s/mm^2 slice was generated by using the snake-based automated segmentation algorithm [8]. The tracking algorithm described here is based of the evaluation of translation invariant first moments (centroid) [9], block matching [10] and active contours [11]. First, the images were normalized to values between 0 and 1. Next, the moments of the lesion described by the contour on the b-450 s/mm^2 slice and by the same contour on the b-300 s/mm^2 slice were calculated. Assuming the average normalized lesion intensities to be the same on both the slices, the displacements along x-direction (δ_x) and the y-direction (δ_y) were calculated as described by Gupta et al. [9]. δ_x and δ_y provided a good estimate of the non-rigid motion associated with the lesion. The contour describing the lesion on the b-450 s/mm^2 slice was shifted onto the b-300 s/mm^2 slice using these estimates. However, this step corrected for just the rigid motion experienced by the lesion, and was not capable of estimating non-rigid motion experienced by the lesion. This was accommodated by allowing the deformation associated with each point on the resulting contour to be determined using block matching. Block matching with a block size of 3 × 3 was applied between corresponding snake points on the contour describing the lesion on the b-450 s/mm^2 slice and the moment-shifted contour on the b-300 s/mm^2 slice. Deformation estimates were generated by block matching using the minimum absolute difference measure. Using these deformation estimates, each point on the contour describing the lesion in the b-300 s/mm^2 slice was shifted to correct for any non-rigid motion. Active contour deformation [11] was applied to this motion-corrected contour to increase the lesion detection accuracy. The whole procedure is then applied to tracking the corresponding lesion on the b-150 s/mm^2 slice, with the contour from the b-300 s/mm^2 slice, as the reference.

Results.

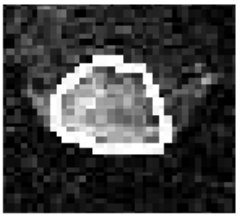

Fig. 1A: Contour on the b-450 data set

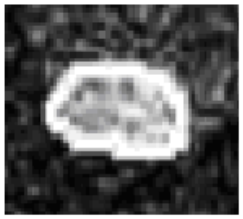

Fig. 1B: Contour on the b-300 data set

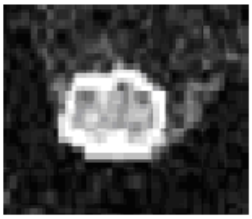

Fig. 1C: Contour on the b-150 data set

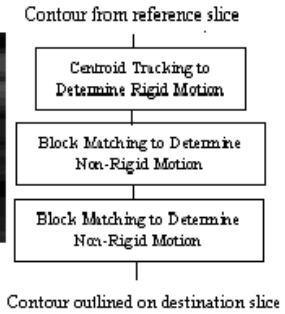

Fig. 2: Block Diagram

Data set	FNR (%)	FPR (%)
b-300 s/mm^2	1.50	1.40
b-150 s/mm^2	3.20	1.70

Table 1: Average FNR and FPR values

Figs. 1A, 1B and 1C show the diffusion-weighted liver images acquired at b-values of 450 s/mm^2, 300 s/mm^2 and 150 s/mm^2, respectively. The images have been cropped and zoomed for better display. Lesion is the bright area in the figure. The contour (shown in white in Fig. 1A) on the b-450 s/mm^2 slice was determined using the automated segmentation algorithm [8]. The motion-tracked contours describing the lesion on the b-300 s/mm^2 and b-150 s/mm^2 slice are shown in Figs. 1B and 1C (shown in white), respectively. Automatically tracked lesions from several data sets were quantitatively compared to data obtained by manual ROI circumscription by a trained radiologist. The false negative ratio (FNR) was calculated as the percentage of lesion pixels in the hand-segmented data that were labeled as non-lesion pixels by the automated scheme. The false positive ratio (FPR) was calculated as the percentage of lesion pixels in the automated assignment that were labeled as non-lesion pixels by the radiologist. The average FNR and FPR values for 17 distinct lesions differing in size and shapes from the b-300 s/mm^2 and b-150 s/mm^2 data sets are shown in table 1. As shown, automated segmentation identified lesions to within 3.2% that of a trained radiologist. Additionally, this algorithm reduced the total time for analysis by a factor of 12, compared to manual segmentation.

Conclusion. This paper describes a method for combining centroid tracking and block matching with the active contour model for liver lesion tracking. The rigid and non-rigid estimates were determined using first moments and block matching respectively. These estimates were used to correct for any rigid or non-rigid motion experienced by the lesion. Active contour deformation was applied to this motion corrected contour to increase lesion detection accuracy. The proposed tracking algorithm is fully automated and requires no user interaction. Results obtained from this algorithm are comparable to those obtained from manual segmentation by a trained radiologist, with a significant reduction in total analysis time.

References. [1] Chenevert, TL et al., Clinical Cancer Res. 1997, pp. 1457-1466. **[2]** Anuta, PF, SPIE J, 1969, pp. 168–175. **[3]** Kumar, S et al., Proc. ICIP, 1996, pp. 359-362. **[4]** Giele, ELW, J of Magn. Resonance Medicine, 2001, pp. 741-749. **[5]** Mikic, I, et al., IEEE Trans Med Imaging, 1998, pp. 274-284. **[6]** Curwen, R, et al., Computer Cardiology, 1994, pp. 109–112. **[7]** Theilmann, RJ, et al., Neoplasia, 2004, in press. **[8]** Krishnamurthy, C, et al., IEEE Proc. SSIAI, 2004, pp. 187-191. **[9]** Gupta, SN, et al., J Magnetic Resonance in Medicine, 2003, pp. 506-513. **[10]** Fernando, J, et al., Proc. Fifth European Sig. Proc. Conf. 1990, pp. 753-756. **[11]** Kass, M, et al., Int. J of Computer Vision, 1987, pp. 321-331.